

NASA TECHNICAL NOTE



NASA TN D-3507

NASA TN D-3507

A PRETENSIONING CONCEPT FOR RELIEF OF CRITICAL LEADING-EDGE THERMAL STRESS

by Jerald M. Jenkins
Flight Research Center
Edwards, Calif.

NATIONAL AERONAUTICS AND SPACE ADMINISTRATION • WASHINGTON, D. C. • JULY 1966

A PRETENSIONING CONCEPT FOR RELIEF OF CRITICAL
LEADING-EDGE THERMAL STRESS

By Jerald M. Jenkins

Flight Research Center
Edwards, Calif.

NATIONAL AERONAUTICS AND SPACE ADMINISTRATION

For sale by the Clearinghouse for Federal Scientific and Technical Information
Springfield, Virginia 22151 – Price \$1.00

A PRETENSIONING CONCEPT FOR RELIEF OF CRITICAL LEADING-EDGE THERMAL STRESS

By Jerald M. Jenkins
Flight Research Center

SUMMARY

The concept of pretensioning high-temperature leading edges is demonstrated. Elementary equations are presented and applied, by means of an example problem, to a mathematical model of a leading-edge system in order to illustrate, analytically, the mechanics of the concept. The results of the example problem show that leading-edge pretensioning significantly reduces the magnitude of critical compressive thermal stress in the leading-edge stagnation region. The general concept of pretensioning offers a new approach to reducing the magnitude of critical operating leading-edge stress. The increased overall margin of safety and the more efficient use of the entire leading-edge cross section is illustrated in the example problem.

INTRODUCTION

The leading edges of lifting and control surfaces of supersonic and hypersonic aircraft experience severe chordwise temperature gradients (ref. 1). The most forward areas of the leading edges reach very high temperatures, while farther downstream the structural temperatures are less severe. This condition induces large spanwise compressive thermal stresses in the stagnation region of the leading edge (refs. 2 to 4). Because of high temperatures, this region is least able to endure stress. The combination of large stress and severe temperature can result in inefficient use of the leading-edge material. Although heat-sink leading edges (ref. 5) reduce chordwise temperature gradients, excessive weight is an undesirable characteristic of this type of leading edge. Thin, segmented leading edges (refs. 6 and 7) have been considered for use at hypersonic speeds; however, chordwise temperature gradients still present a major problem.

This paper introduces an analytical concept designed to relieve problems arising from the chordwise temperature gradients by reducing the magnitude of critical compressive stress in a leading edge. The reduction is accomplished by adding an internal column (referred to herein as a pretensioning component) that applies an internal load to the ends of the leading edge. Equations that define the behavior of a pretensioned leading edge are developed and applied to a mathematical model to demonstrate the mechanics of using the concept.

The pretensioning concept is presented in an elementary manner for two primary reasons: (1) A more sophisticated approach would require the derivation of extensive equations in order to present the concept. The object of this paper is to present the pretensioning concept itself in a comprehensive manner, rather than to apply the concept to a unique leading-edge configuration. (2) There is no unique leading-edge structural configuration in general use; hence, for particular applications, leading-edge geometries will vary radically. The extent to which the exact stress analysis must be obtained will, correspondingly, depend upon the configuration selected. Therefore, no specific configuration is associated with the development of the equations.

SYMBOLS

The units used for the physical quantities in this paper are given both in the International System of Units (SI) and the U. S. Customary Units. Factors relating the two systems are given in reference 8.

A	area, centimeter ² (inch ²)
a	arbitrary dimension
E	Young's modulus, newtons/meter ² (pounds/inch ²)
F	initial equilibrium force, newtons (pounds)
F'	instantaneous equilibrium force, newtons (pounds)
I	moment of inertia, centimeter ⁴ (inch ⁴)
K	constant for temperature expression, degrees Kelvin/centimeter ² (degrees Fahrenheit/inch ²)
l	half length, centimeters (inches)
T	temperature, degrees Kelvin (degrees Fahrenheit)
t	time, seconds
u	axial displacement in x-direction
u _F	initial leading-edge-system displacement to attain static equilibrium, centimeters (inches)
u' _F	instantaneous displacement defining the equilibrium position of a heated leading-edge system, centimeters (inches)
u _m	unrestrained displacement of the leading edge due to heating of the com- ponent, centimeters (inches)

u_p	unrestrained displacement of the pretension component due to heating, centimeters (inches)
$u(t)$	time-dependent displacement, centimeters (inches)
x, y, z	Cartesian coordinate axes
x_1	reference axis passing through center of undeformed pretension component
y_e	eccentricity of pretension component, centimeters (inches)
α	coefficient of thermal expansion, centimeter/centimeter degrees Kelvin (inch/inch degrees Fahrenheit)
Δ_e	rotational error of the leading-edge displacement, centimeters (inches)
Δ_0	initial difference in half lengths of the leading edge and pretension component, centimeters (inches)
Δ'_0	instantaneous difference in the unrestrained lengths of the leading edge and the pretension component, centimeters (inches)
ϵ	strain, centimeter/centimeter (inch/inch)
σ	stress, newtons/meter ² (pounds/inch ²)
Subscripts:	
m	leading edge
p	pretension component
R	resultant stress obtained from the algebraic sum of the individual stress components
T	temperature effect
x, z	refer to x- and z-directions, respectively
Y	yield value

ANALYSIS

A generalized leading-edge system, including the reference axes, is shown in figure 1. The x-axis is located coincident with the neutral axis of the leading-edge system. A component used for pretensioning is eccentrically located from the x-axis a distance y_e ; the axis of the component is also in the x-y plane. Excluding the

pretension component, the remainder of the leading-edge system will, hereafter, be referred to as the leading edge. The following specific assumptions pertinent to the analysis of the leading-edge system are made:

1. The cross section of the leading-edge system is uniform in the x -direction.
2. The temperature varies only in the y -direction.
3. The distribution of thermal stress is uniform in the x - and z - directions.
4. The y - and z -axes are the principal and neutral axes of the cross section.
5. The cross-sectional area of the pretension component is small compared to that of the leading edge. This area is neglected in calculations involving the leading edge.
6. There is no friction between the pretension component and the leading edge. The two components are integrated only by bearing at the ends of the pretension component.
7. The centroid of the pretension component is in the x - y plane.

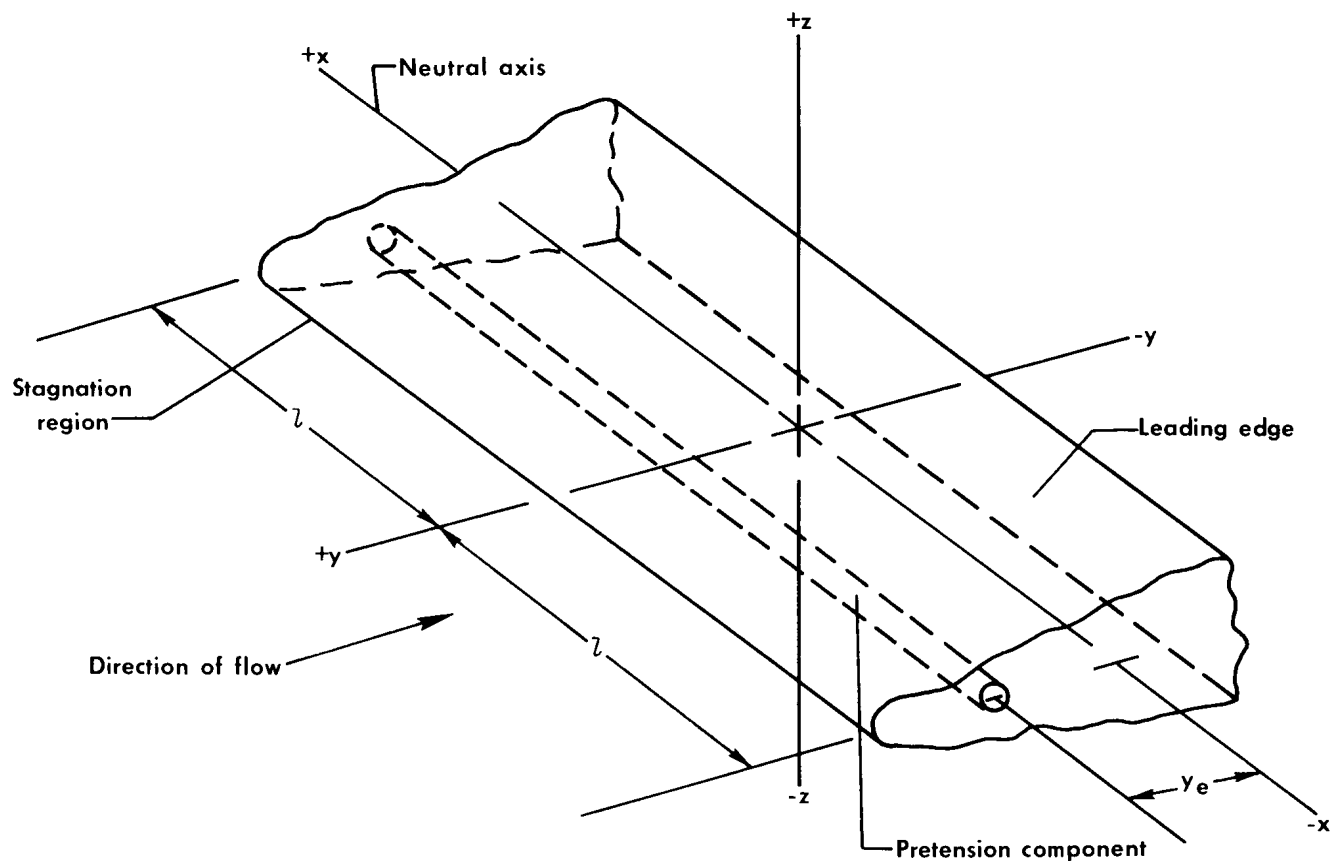


Figure 1.— Generalized leading-edge system with a pretension component.

The thermal stress in the unrestrained leading edge can be computed according to conventional beam-theory techniques. It has been shown (ref. 3) that such techniques provide reasonably accurate values of stresses. If the thermal stress is compatible with the preceding assumptions and with the assumptions in reference 9 for the unrestrained leading edge (see appendix A for complete derivation of eq. (1)), it can be computed from the following equation (refs. 9 and 10)

$$\sigma_T = -E_m \alpha_m T + \frac{\int_{A_m} E_m \alpha_m T dA_m}{\int_{A_m} dA_m} + \frac{\int_{A_m} E_m \alpha_m T y dA_m}{\int_{A_m} y^2 dA_m} y \quad (1)$$

The temperature distribution of an aircraft structure cannot be defined practically as a concise mathematical expression, and equation (1) cannot be directly integrated. The conventional procedure used for such cases is to approximate the integrals by numerical methods.

Initially, the leading edge will be considered to have an unstressed half length l , and the pretension component will have a slightly longer unstressed half length $l + \Delta_0$ (see fig. 2(a)). It should be noted in the development of the subsequent equations that all displacements and dimensions in the x-direction are measured along the axis of the pretension component (i.e., the $x_1 - x_1$ axis). If the pretension component is compressed an amount Δ_0 and is held in such a position, the two components will have an identical half length (fig. 2(b)). By attaching the two components according to assumption 6 and then releasing them, the components will assume some position of static equilibrium defined by the dashed lines and the displacement u_F in figure 2(c).

If F represents the force in the pretension component in the equilibrium position, then

$$\sigma_m = F \left(\frac{y_e y}{I_m} + \frac{1}{A_m} \right) \quad (2)$$

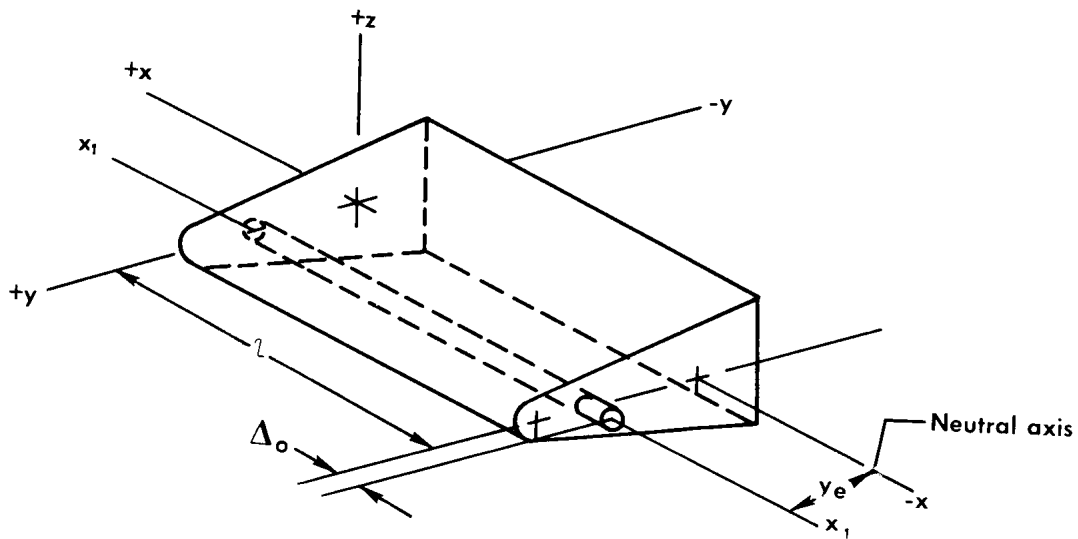
and

$$\sigma_p = -\frac{F}{A_p} \quad (3)$$

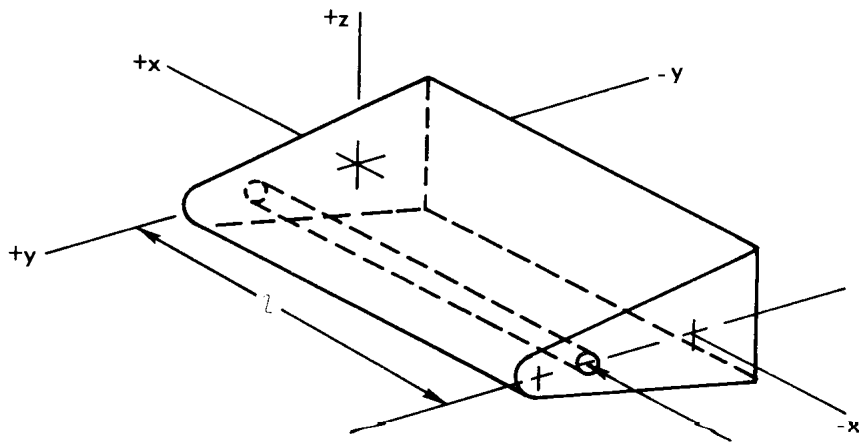
where σ_m is the stress in the leading edge and σ_p is the stress in the pretension component.

In the equilibrium position, the pretension component has been compressed by an amount $\Delta_0 - u_F$, and the leading edge has displaced an amount u_F . Using Hooke's law

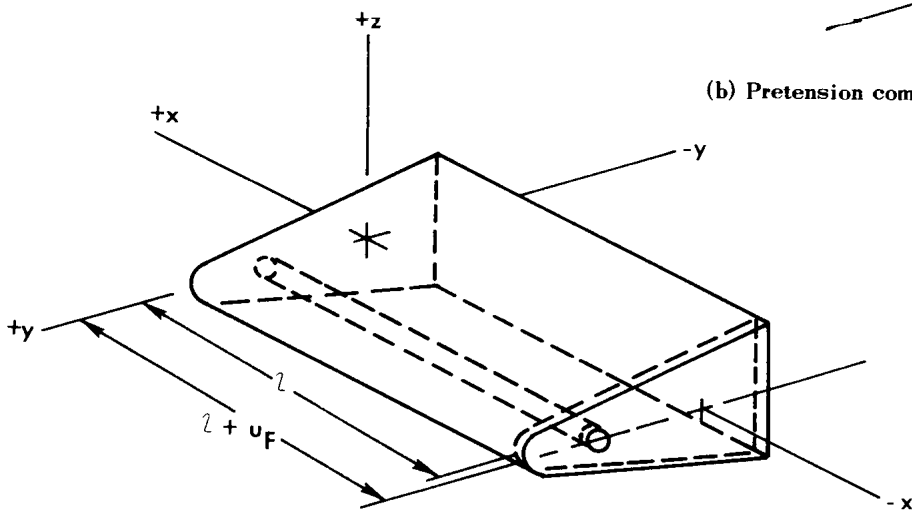
$$\Delta_0 - u_F = \frac{F l_p}{A_p E_p} \quad (4)$$



(a) Initial unstressed half length.



(b) Pretension component is compressed and held.



(c) Two components are attached, then released.

Figure 2.— Mechanics of leading-edge pretensioning.

and the mechanics of bending

$$u_F = \frac{Fl_m}{E_m} \left(\frac{y_e^2}{I_m} + \frac{1}{A_m} \right) \quad (5)$$

Equations (4) and (5) may be solved simultaneously for F and u_F . Once the equilibrium force F is thus established, the stress distribution in the two components may be found by solving equations (2) and (3).

The state of stress in the leading-edge system will be changing during flight as a result of the presence of transient thermal stress induced by aerodynamic heating. It is necessary, therefore, to develop expressions for the resultant stress and the displacement during the period of transient heating.

The concept can best be explained by considering the unrestrained translations of the individual components resulting from temperature changes. The unrestrained displacement of the leading edge in the x -direction due to this translation is represented by u_m in figures 3(a) to 3(d). The temperature rise in the unrestrained pre-tension component will lead to an elongation u_p in addition to the initial length $l + \Delta_o$. Therefore, during a heating situation, the total unrestrained displacement of the leading edge is represented by u_m and the unrestrained displacement of the pre-tension component is u_p . Therefore, at any instant of time, the difference in the unrestrained lengths Δ'_o of the two components is

$$\Delta'_o = (\Delta_o + u_p) - u_m \quad (6)$$

However, since the two components are not unrestrained but are attached, they will reach a position of static equilibrium defined by u'_F . Now that the instantaneous difference in the unrestrained lengths Δ'_o and the equilibrium displacement u'_F are defined, relationships between these quantities and the internal forces can be established.

Using Hooke's law and the mechanics of bending, the expressions relating u'_F and the instantaneous force between the two components F' are

$$\Delta'_o - u'_F = \frac{F' l_p}{A_p E_p} \quad (7)$$

$$u'_F = \frac{F' l_m}{E_m} \left(\frac{y_e^2}{I_m} + \frac{1}{A_m} \right) \quad (8)$$

The displacements u_p and u_m may be expressed by the following equations (ref. 9)

$$u_p = \alpha_p l_p T \quad (9)$$

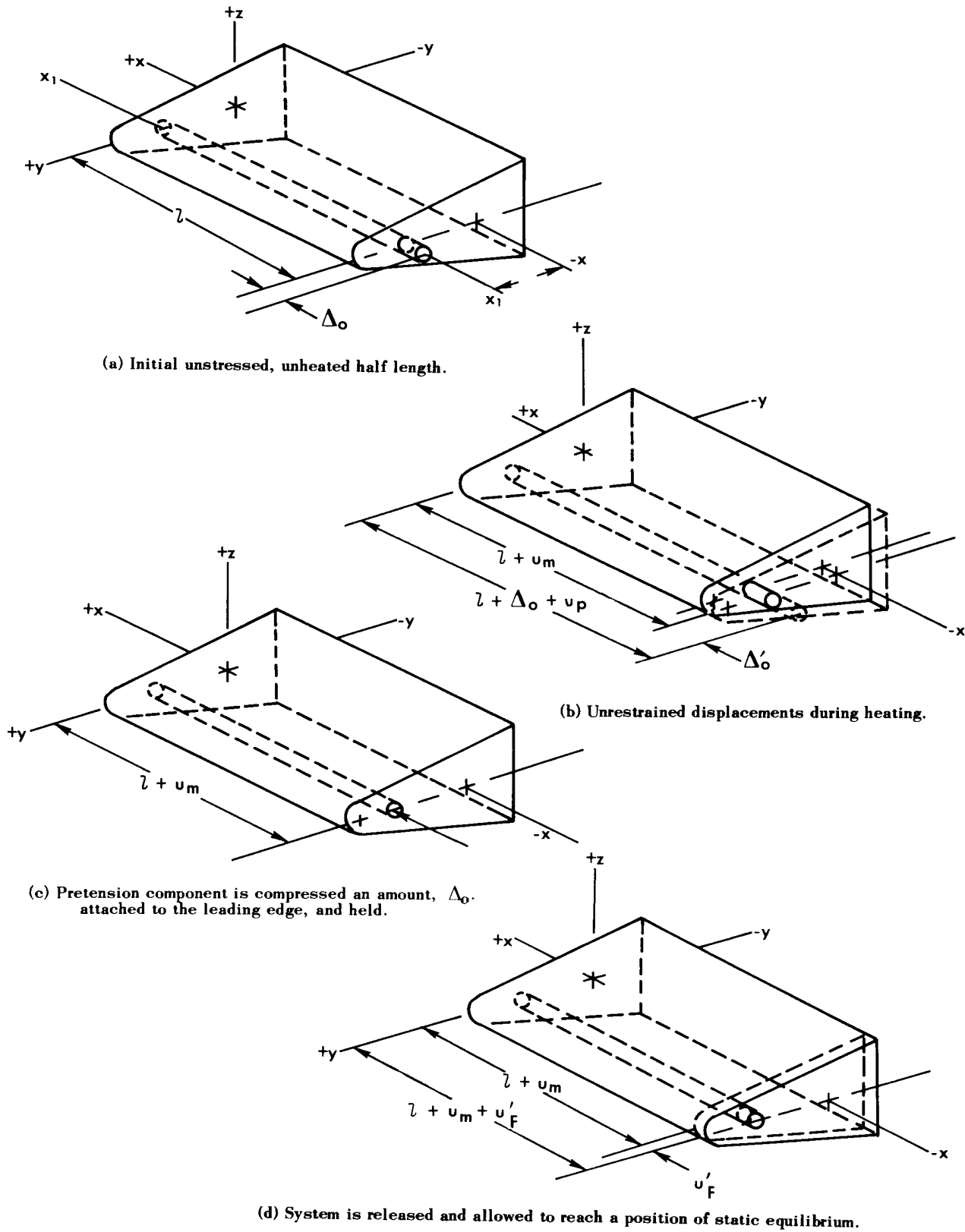


Figure 3.— Mechanics of leading-edge pretensioning with heating included.

$$u_m = \int_0^l \left[\frac{\int_{A_m} \alpha_m T dA_m}{\int_{A_m} dA_m} + \frac{\int_{A_m} \alpha_m T y dA_m}{\int_{A_m} y^2 dA_m} y \right] dx \quad (10)$$

It should be noted that equation (9) represents the axial displacement of the pre-tensioning component. No correction is included for the rotation of this component when it is attached to the leading edge. This problem is discussed in detail in appendix B. Substitution of equations (9) and (10) into equation (6) yields

$$\Delta_o + \alpha_p l_p T - u'_F - \int_0^l \left[\frac{\int_{A_m} \alpha_m T dA_m}{\int_{A_m} dA_m} + \frac{\int_{A_m} \alpha_m T y dA_m}{\int_{A_m} y^2 dA} y \right] dx = \frac{F' l_p}{E_p A_p} \quad (11)$$

The terms in equation (11) that express either displacements or material properties vary with temperature, and, since the temperature varies with time, the terms are, in reality, functions of time. To simplify the derivation, material properties (α and E) are treated as constants. Displacements (u_p and u_m) are retained as time-dependent terms and are written hereafter as $u_p(t)$ and $u_m(t)$. Equations (6), (7), and (8) may be combined to obtain the following expression for F' , the load in the pretension component

$$F' = \frac{\Delta_o + u_p(t) - u_m(t)}{\frac{l_p}{E_p A_p} + \frac{l_m}{E_m} \left(\frac{y_e^2}{I_m} + \frac{1}{A_m} \right)} \quad (12)$$

Stress equations are obtained by substituting the load from equation (12) into equations (2) and (3) as follows

$$\sigma_m = \frac{\left(\frac{y_e y}{I_m} + \frac{1}{A_m} \right) [\Delta_o + u_p(t) - u_m(t)]}{\left[\frac{l_p}{E_p A_p} + \frac{l_m}{E_m} \left(\frac{y_e^2}{I_m} + \frac{1}{A_m} \right) \right]} \quad (13)$$

$$\sigma_p = - \left[\frac{\Delta_o + u_p(t) - u_m(t)}{A_p} \right] \left\{ \frac{1}{\left[\frac{l_p}{E_p A_p} + \frac{l_m}{E_m} \left(\frac{y_e^2}{I_m} + \frac{1}{A_m} \right) \right]} \right\} \quad (14)$$

Equations (13) and (14) are general expressions for the transient stress throughout the integral system. The magnitude of stress may be controlled by varying the initial pretension input Δ_0 . Current engineering capabilities allow a reasonably accurate preflight prediction of aerodynamic heating for a prescribed flight profile. Thus, the magnitude of thermal stress as well as the time at which critical stress occurs may be computed in advance. Once this information has been established, an initial pretension input Δ_0 can be determined by superimposing (ref. 11) the stresses of equations (1) and (13) and equating the sum to zero. The resulting expression is then solved for the Δ_0 required to reduce the resulting stress σ_R to zero at the value of y corresponding to the critical stress, as follows

$$\sigma_R = 0 = \frac{\left(\frac{y e^y}{I_m} + \frac{1}{A_m}\right) [\Delta_0 + u_p(t) - u_m(t)]}{\left[\frac{l_p}{E_p A_p} + \frac{l_m}{E_m} \left(\frac{y e^2}{I_m} + \frac{1}{A_m}\right)\right]} - E_m \alpha_m T + \frac{\int_{A_m} E_m \alpha_m T dA_m}{\int_{A_m} dA_m} + \frac{\int_{A_m} E_m \alpha_m T y dA_m}{\int_{A_m} y^2 dA_m} y \quad (15)$$

Further evaluation of a specific leading-edge problem may lead the designer to consider only partial pretensioning in order to create an even more favorable stress pattern than defined in the preceding equations.

ILLUSTRATIVE EXAMPLE

In order to demonstrate the advantage of redistributing stress by pretensioning, an example problem will be solved using a solid wedge-shaped leading edge. The computations are nondimensionalized for purposes of simplification. One-half of the leading edge is shown in figure 4, with relative dimensions and material properties indicated. It is required that the leading edge operate in a thermal environment in which the temperature is defined by the equation

$$T = K e^t (y + a)^2 \quad (16)$$

and the time interval is

$$0 \leq t \leq 6 \quad (16a)$$

Since the temperature is assumed to be uniform in the x - and z -directions and the component has significant length, a thermal-stress analysis of the wedge can be made for the given temperature environment by using equation (1)

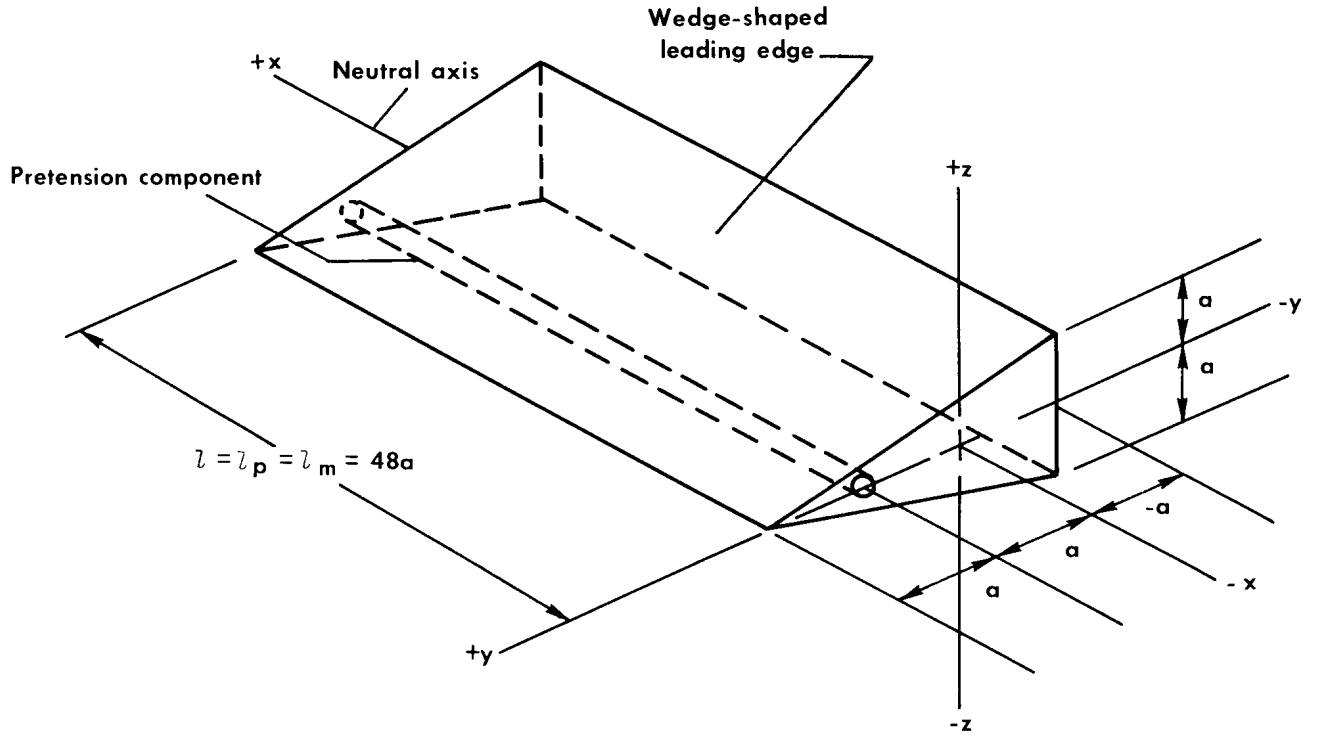


Figure 4.— Mathematical model of a leading edge. $\alpha_m = \alpha_p$; $A_p = \frac{a^2}{9}$; $A_m = 3a^2$; and $I_z = \frac{3}{2}a^4$.

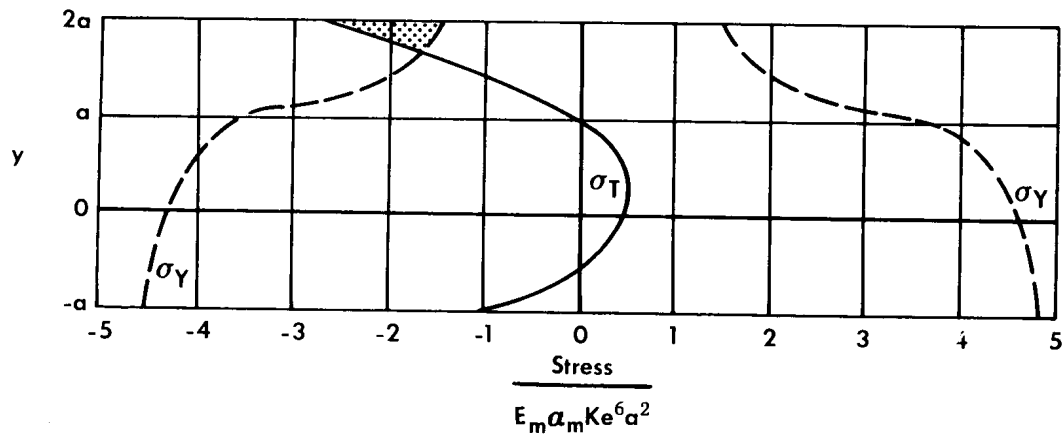
$$\sigma_T = -E_m \alpha_m Ke^t (y + a)^2 + \frac{\frac{2}{3} \int_{-a}^{2a} E_m \alpha_m Ke^t (y + a)^2 (2a - y) dy}{\frac{2}{3} \int_{-a}^{2a} (2a - y) dy} + \frac{\frac{2}{3} \int_{-a}^{2a} E_m \alpha_m Ke^t (y + a)^2 (2a - y) y dy}{\frac{2}{3} \int_{-a}^{2a} (2a - y) y^2 dy} y \quad (17)$$

The thermal stress, calculated by using equation (17), is shown in figure 5 for $t = 6$ seconds as a function of y . As shown, the maximum value of thermal stress occurs at $y = 2a$, and the magnitude is

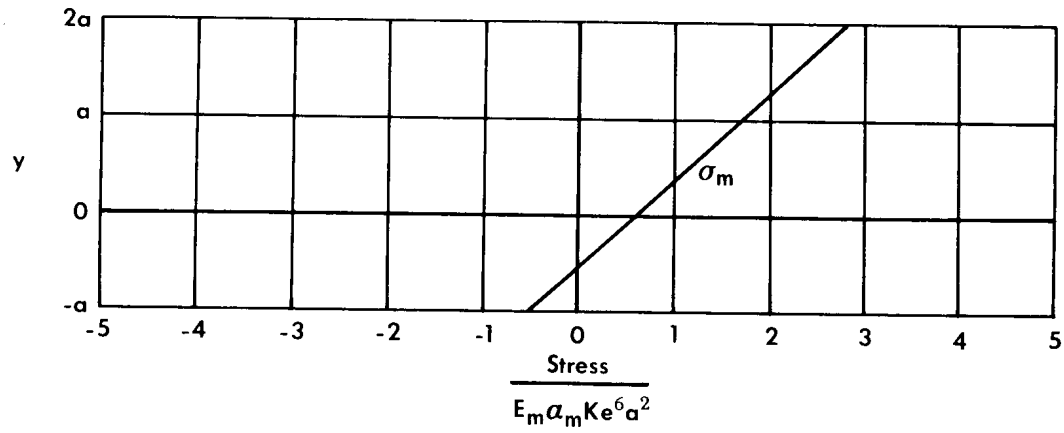
$$\sigma_T = -\frac{27}{10} E_m \alpha_m Ke^6 a^2 \quad (18)$$

It is assumed that at $t = 6$ seconds the heating cycle ends and uniform cooling occurs.

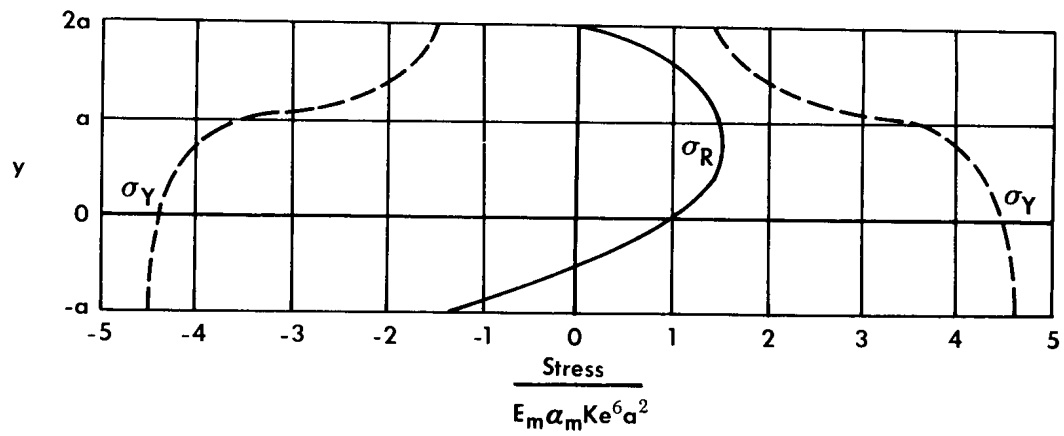
Since the yield strength of the wedge material varies with temperature and the temperature varies in the y -direction, the yield strength is also a function of y . This relationship is represented by the dashed lines in figure 5. The yield strength of the



(a) Nondimensional thermal stress, σ_T .



(b) Nondimensional pretension stress, σ_m .



(c) Nondimensional resultant stress, σ_R .

Figure 5.— Nondimensional stress components of wedge-shaped leading edge. $t = 6$ sec.

wedge material for $t = 6$ seconds is illustrated on the positive horizontal axis, and the compressive yield strength of the wedge material is illustrated on the negative horizontal axis. The thermal stress σ_T is also shown in the figure for $t = 6$ seconds. It can be seen that the thermal stress exceeds the yield strength of the wedge material near the stagnation region of the leading edge. This compressive yielding is represented by the shaded area.

Since the magnitude, location, and time of maximum thermal stress have been determined and since it is further known that the anticipated thermal environment will cause yielding of the wedge material, it is now appropriate to correct this situation by utilizing a pretension mechanism. As shown in figure 4, a pretension component is located a distance $y_e = a$ from the neutral axis. The pretension component is assumed to be mechanically capable of transmitting concentrated forces to the leading edge, according to assumption 6. For simplification, only the positive x-half of the wedge is considered, as shown in figure 4.

A pretension input Δ_0 is determined such that the maximum thermal stress is reduced to zero. This input can be computed by first solving the transient forms of equations (9) and (10) at the time of maximum thermal stress, then substituting these values into equation (15), and finally solving this equation for Δ_0 as follows

$$u_p(t) = \int_0^{48a} \alpha_p K e^t (y + a)^2 dx \quad (19)$$

$$u_p(6) = \frac{1920}{10} \alpha_p K e^6 a^3 \quad (19a)$$

$$u_m(t) = \int_0^{48a} \left[\frac{\int_{-a}^{2a} \alpha_m K e^t (y + a)^2 (2a - y) dy}{\int_{-a}^{2a} (2a - y) dy} + \frac{\int_{-a}^{2a} \alpha_m K e^t (y + a)^2 (2a - y) y dy}{\int_{-a}^{2a} (2a - y) y^2 dy} y \right] dx \quad (20)$$

$$u_m(6) = \frac{1872}{10} \alpha_m K e^6 a^3 \quad (20a)$$

The initial pretension input Δ_0 is

$$\Delta_0 = \frac{81}{50} E_m \alpha_m K e^6 a^3 \left(\frac{432}{E_p} - \frac{48}{E_m} \right) - \frac{48}{10} \alpha_m K e^6 a^3 \quad (21)$$

If a pretension input of the magnitude given by equation (21) is applied before the wedge is used in the thermal environment, a leading-edge stress will be present at the time of maximum thermal stress, as a result of pretensioning, which is equal in magnitude but opposite in sign to the maximum thermal stress.

The stress component at the critical time due to the pretensioning of the wedge can be determined by first computing the force in the pretension component according to equation (12) and substituting this value into equation (13). Therefore

$$F' = \frac{81}{50} E_m \alpha_m K e^{6a^4} \quad (22)$$

$$\sigma_m = \frac{81}{50} E_m \alpha_m K e^{6a^4} \left(\frac{y e y}{I_m} + \frac{1}{A_m} \right) \quad (23)$$

The results of the example problem are shown in figures 5(a), (b), and (c). It was found that the thermal stress σ_T for a given temperature environment was of sufficient magnitude to cause compressive yielding of the leading edge. The maximum value, the location, and the time of occurrence of this critical compressive thermal stress were then determined. The pretensioning concept was applied, and an initial pretension input Δ_0 was determined such that the critical compressive thermal stress was reduced to zero at the time and location of the maximum thermal stress. Figure 5(c) further illustrates that the resultant stress σ_R , which was obtained by superimposing the thermal stress σ_T upon the component of stress caused by pretensioning σ_m , only slightly increased the levels of resultant stress in other regions of the leading edge. The areas in which these increases occurred, however, still remain far below either the compressive or tensile yield strength of the leading-edge material.

DISCUSSION

The pretensioning concept has been analytically demonstrated on a mathematical model of a leading edge that was required to operate in a thermal environment of such severity that compressive yielding of the material would occur. The pretensioning concept was then applied, and the resulting stress distribution graphically illustrated that the overall margin of safety of the leading edge was greatly increased for that particular operating environment.

The foregoing example problem illustrates, analytically, that, by mechanical pretensioning procedures, critical thermal stresses can be redistributed in such a manner that no stress approaches the yield limit of the material. An even more severe thermal environment could be withstood by varying the initial pretension deformation Δ_0 by an appropriate amount.

The limiting capacity of a pretensioned leading-edge system is governed by several factors. The geometry of the leading edge and the location and size of the pretension component are parameters that can be used for purposes of weight optimization. The availability of a large variety of feasible high-temperature materials provides the designer with innumerable combinations of mechanical properties to utilize in an efficient leading-edge design. Inasmuch as the ratio of A_p/A_m

would be very small, a probable limiting factor of the system would be the compressive yield strength of the pretension component. In addition, the same effect as pretensioning may be accomplished by selecting two materials for use which have radically differing coefficients of thermal expansion. The differential growth of the two materials during heating would result in internal tensioning of the leading edge. Since application of the pretensioning concept results in a redistribution of stress, radical leading-edge geometries and brittle materials should be examined for modes of failure due to overstressing by pretensioning.

Other problems that may influence the successful application of the pretensioning concept must be investigated for each unique leading-edge configuration. The pretension device must be incorporated in the leading edge in such a manner as to avoid stress-concentration problems. In addition, the high operating temperature of a leading-edge structure could introduce creep problems if the pretension device is operated at excessive stress levels.

The equilibrium equations were derived on the basis of the assumption that the distribution of thermal stress σ_T was uniform in the x-direction. However, it is known that thermal stress in an elastic body must attenuate to zero at a boundary free of surface tractions in order to satisfy the conditions of surface equilibrium. An example of this phenomenon is reported in reference 12. Although published information does not specifically define the nature of this attenuation for leading-edge geometries, some allowance must be made when the part of the leading-edge length to be pretensioned is selected. If the full length of the leading edge is pretensioned, a failure might occur in the end regions of the leading edge at elevated temperature because of the combined effects of the pretension load, the deteriorated strength of the material, and the absence of thermal stress. It will be necessary, therefore, to pretension only the regions of the leading edge remote from the ends. In view of the lack of knowledge of the distribution of thermal stress in the vicinity of the leading-edge ends, the most logical solution is to determine experimentally the distance from the ends of the leading edge at which the thermal-stress attenuation becomes negligible. Once this distance is determined for a particular leading-edge configuration, only the region in which thermal-stress attenuation is negligible should be considered for pretensioning.

CONCLUDING REMARKS

The concept of pretensioning high-temperature leading edges was demonstrated. Pretensioning was accomplished by adding an eccentric internal structural component capable of transmitting a combined axial and bending load to the leading edge in the spanwise direction. Elementary equations were presented and applied, by means of an example problem, to a mathematical model of a leading-edge system in order to demonstrate, analytically, that leading-edge pretensioning significantly reduces the magnitude of critical compressive thermal stress in the leading-edge stagnation region.

The large variety of high-temperature materials currently available offers the designer many combinations of mechanical properties with which to effect an efficient leading-edge design by using the pretensioning concept. The redistribution of

leading-edge stresses due to pretensioning should be examined for adverse effects when the concept is applied to radical leading-edge geometries. Specific information defining thermal-stress attenuation near the end regions of unique leading-edge configurations is not available.

The general concept of pretensioning offers a new approach to reducing the magnitudes of critical operating leading-edge stresses. The increased overall margin of safety and the more efficient use of the entire leading-edge cross section was illustrated in an example problem.

Flight Research Center,
National Aeronautics and Space Administration,
Edwards, Calif., April 6, 1966.

APPENDIX A

DERIVATION OF THE MODIFIED THERMAL-STRESS EQUATION

The basic approach used to develop the equations for thermal stress (eq. (1)) has been modified in this paper to include simplifying assumptions. The manner in which these assumptions are included in the thermoelastic beam-theory approach to establish stress expressions is developed in this appendix.

Using the coordinate system shown in figure 1, the derivation will be initiated by assuming the Bernoulli-Euler assumption to be valid. It will be further assumed that Poisson's ratio is zero and that the leading edge is free of external loads. The axial displacement u (x-direction) must be a linear function of the y - and z - coordinates. Hence, the axial displacement may be written in the form

$$u = g_0(x) + yg_1(x) + zg_2(x) \quad (A1)$$

The normal strain in the x-direction is

$$\epsilon_x = \frac{\partial u}{\partial x} = g'_0(x) + yg'_1(x) + zg'_2(x) \quad (A2)$$

The expression for stress, using the simplified form of Hooke's law, is

$$\sigma_x = E(\epsilon_x - \alpha T) = E[g'_0(x) + yg'_1(x) + zg'_2(x) - \alpha T] \quad (A3)$$

Assumption 2 (page 4) provides that the temperature does not vary in the x-direction; hence, the coefficients, $g'_0(x)$, $g'_1(x)$, and $g'_2(x)$ must be constants and will, henceforth, be referred to as g_0 , g_1 , and g_2 , respectively. These constants must be determined according to the following conditions of static equilibrium

$$\int_A \sigma_x dA = 0 \quad (A4)$$

$$\int_A \sigma_x y dA = 0 \quad (A5)$$

$$\int_A \sigma_x z dA = 0 \quad (A6)$$

The expression for the axial stress is now

$$\sigma_x = E(g_0 + yg_1 + zg_2 - \alpha T) \quad (A7)$$

By substituting equation (A3) into equations (A4), (A5), and (A6), the following set of simultaneous equations for the unknown constants, g_0 , g_1 , and g_2 , is obtained

$$\left. \begin{aligned} g_0 \int_A dA + g_1 \int_A y dA + g_2 \int_A z dA &= \int_A \alpha T dA \\ g_0 \int_A y dA + g_1 \int_A y^2 dA + g_2 \int_A y z dA &= \int_A \alpha T y dA \\ g_0 \int_A z dA + g_1 \int_A z y dA + g_2 \int_A z^2 dA &= \int_A \alpha T z dA \end{aligned} \right\} \quad (A8)$$

Assumption 4 provides that the y - and z -axes are the principal and neutral axes. Therefore, the following terms of equations (A8) must be zero

$$\int_A y dA = \int_A z dA = \int_A y z dA = 0 \quad (A9)$$

Then, equations (A8) reduce to

$$\left. \begin{aligned} g_0 \int_A dA &= \int_A \alpha T dA \\ g_1 \int_A y^2 dA &= \int_A \alpha T y dA \\ g_2 \int_A z^2 dA &= \int_A \alpha T z dA \end{aligned} \right\} \quad (A10)$$

Assumption 2 provides that the temperature does not vary in the z -direction, hence

$$\int_A \alpha T z dA = 0 \quad (A11)$$

and

$$g_2 = 0 \quad (A12)$$

Therefore, equation (A10) may be used to solve for the values of g_0 and g_1

$$\left. \begin{aligned} g_0 &= \frac{\int_A \alpha T dA}{\int_A dA} \\ g_1 &= \frac{\int_A \alpha T y dA}{\int_A y^2 dA} \end{aligned} \right\} \quad (A13)$$

Substituting equations (A12) and (A13) into equation (A7), the expression for the axial stress becomes

$$\sigma_x = E \left(\frac{\int_A \alpha T dA}{\int_A dA} + \frac{\int_A \alpha T y dA}{\int_A y^2 dA} y - \alpha T \right) \quad (A14)$$

or

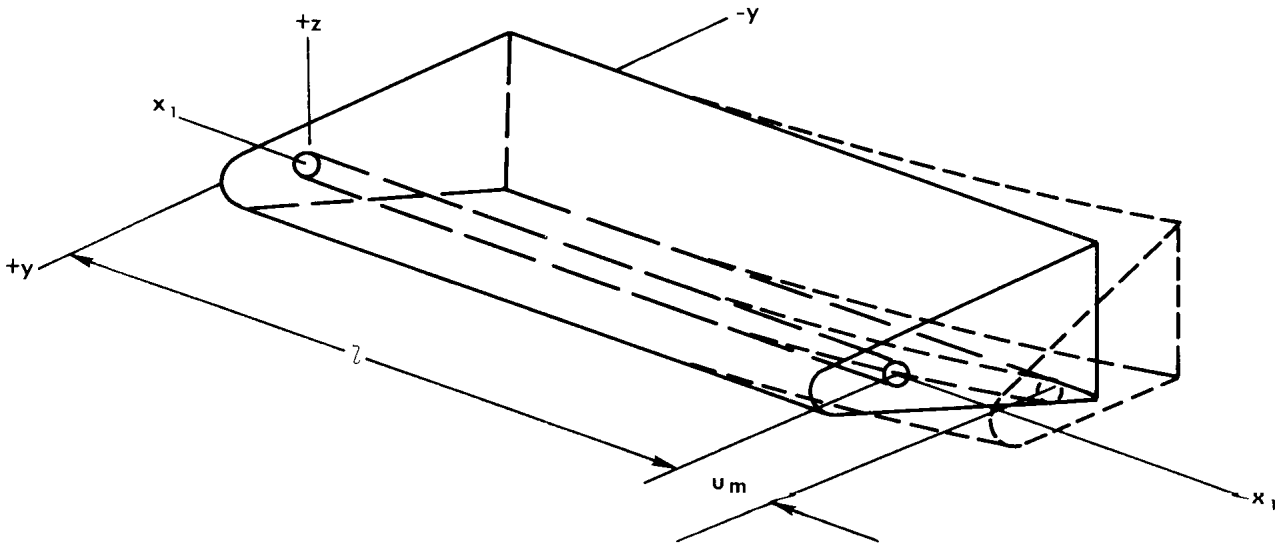
$$\sigma_x = -E\alpha T + \frac{\int_A E\alpha T dA}{\int_A dA} + \frac{\int_A E\alpha T y dA}{\int_A y^2 dA} y \quad (A15)$$

Equation (A15), the expression for the thermal stress in the x-direction, is identical in form to equation (1).

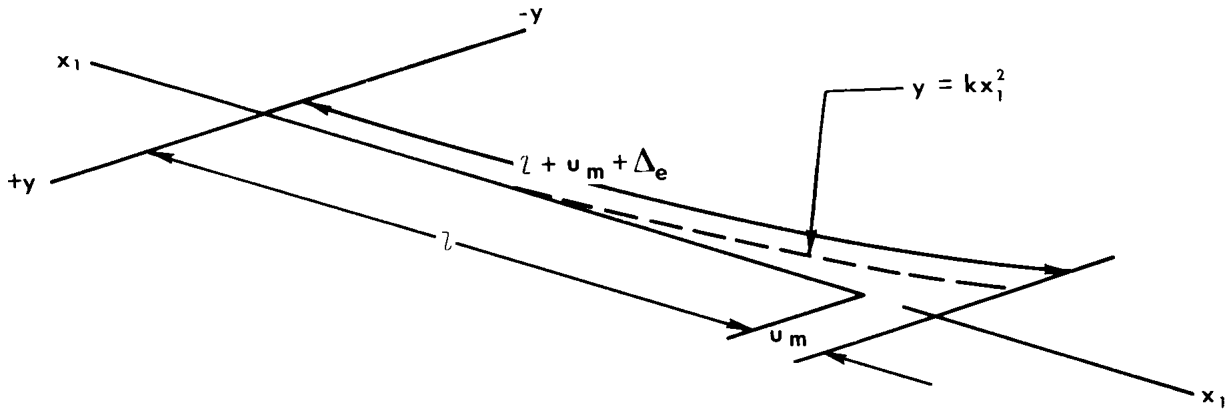
APPENDIX B

POTENTIAL SOURCES OF ERROR

The equilibrium equations (eqs. (4) and (5)) contain an error that can be significant for large pretension component eccentricities or large thermal bending moments. It should be recalled that the pretension component deformation u_p represented the elongation of the pretension component caused by an increase in temperature. This deformation is measured along the axis of the pretension component, which would be a curved line in the case of the nonuniform temperature distribution. The deformation of the leading edge u_m used in the development of the equilibrium equations is not measured along the axis of the pretension component but along the x -reference axis (fig. 6(a)). Therefore, if the thermal bending moment or pretension eccentricity is large enough, a correction Δ_e (fig. 6(b)) must be included in the equilibrium equations.



(a) Thermally deflected shape of a typical leading edge.



(b) Thermally deflected shape of pretension component axis.

Figure 6.— Rotational error of leading-edge system.

Since no longitudinal temperature variation is being considered, it follows that the unrestrained deformation of the leading edge is of general parabolic form. If the deformation from a reference axis x_1 (fig. 6) follows an expression such as $y = Kx_1^2$, the error Δ_e can be expressed as

$$\Delta_e = \int_0^{l+u_m} \sqrt{l + 4K^2x_1^2} \, dx_1 - (l + u_m) \quad (B1)$$

or

$$\begin{aligned} \Delta_e = K \left[(l + u_m) \sqrt{\frac{1}{4K^2} + (l + u_m)^2} \right. \\ \left. + \frac{1}{4K^2} \log \left| 2K(l + u_m) + \sqrt{1 + 4K^2(l + u_m)^2} \right| \right] - (l + u_m) \end{aligned} \quad (B2)$$

This error is usually negligible; however, its relative magnitude can be determined easily by solving equation (B2). If the error Δ_e is found to be significantly large, it must be added to u_m in equations (8), (10), and (11).

An additional error results from the use of equation (10) to compute the displacement of the leading edge by thermoelastic beam theory. Since the pretensioning concept is to be applied to problems involving inelastic yielding of the leading edge, the extent to which plastic displacement affects the longitudinal displacement should be investigated if large plastic deformations are anticipated.

An inefficiency may exist in some pretensioning mechanisms that could lead to errors. The magnitude of this error, which could be significant, can be determined by a mechanical calibration.

REFERENCES

1. Watts, Joe D.; and Banas, Ronald P.: X-15 Structural Temperature Measurements and Calculations for Flights to Maximum Mach Numbers of Approximately 4, 5, and 6. NASA TM X-883, 1963.
2. Becker, John V.: The X-15 Project. Astronaut. Aeron., vol. 2, no. 2, Feb. 1964, pp. 52-61.
3. Anthony, Frank M.; Merrihew, Fred A.; Mistretta, Andrew L.; and Dukes, Wilfred H.: Investigation of Feasibility of Utilizing Available Heat-Resistant Materials for Hypersonic Leading Edge Applications. Vol. I - Summary. Tech. Rep. 59-744, Wright Air Dev. Center, U. S. Air Force, Jan. 1961.
4. Anthony, F. M.; Blessing, A. H.; Buckley, W. H.; and Dukes, W. H.: Investigation of Feasibility of Utilizing Available Heat Resistant Materials for Hypersonic Leading Edge Applications. Vol. II - Analytical Methods and Design Studies. Tech. Rep. 59-744, Wright Air Dev. Center, U. S. Air Force, Mar. 1961. (Available from ASTIA as AD 265 083.)
5. Kordes, Eldon E.; Reed, Robert D.; and Dawdy, Alpha L.: Structural Heating Experiences on the X-15 Airplane. NASA TM X-711, 1962.
6. Anderson, Melvin S.; Trussell, Donald H.; and Stroud, C. W.: Research on Radiation Heat Shields for Bodies and Leading Edges. NASA TM X-312, 1960.
7. Jenkins, Jerald M.; and Sefic, Walter J.: Experimental Investigation of Thermal-Buckling Characteristics of Flanged, Thin-Shell Leading Edges. NASA TN D-3243, 1966.
8. Mechtly, E. A.: The International System of Units - Physical Constants and Conversion Factors. NASA SP-7012, 1964.
9. Boley, Bruno A.; and Weiner, Jerome H.: Theory of Thermal Stresses. Second ed., John Wiley & Sons, Inc., 1962.
10. Switzky, H.; Forray, M. J.; and Newman, M.: Thermo-Structural Analysis Manual. Vol. I. Tech. Rep. No. WADD-TR-60-517, Wright Air Dev. Div., U. S. Air Force, Aug. 1962.
11. Timoshenko, S.; and Goodier, J. N.: Theory of Elasticity. Second ed., McGraw-Hill Book Co., Inc., 1951, pp. 235-236.
12. Heldenfels, Richard R.; and Roberts, William M.: Experimental and Theoretical Determination of Thermal Stresses in a Flat Plate. NACA TN 2769, 1952.